Combustion and Flame 173 (2016) 99–105

Contents lists available at ScienceDirect

Combustion and Flame

journal homepage: www.elsevier.com/locate/combustflame

Theoretical and numerical analysis of oscillating diffusion flames

Milan Miklavčič[a,*], Indrek S. Wichman[b]

[a] Department of Mathematics, Michigan State University, East Lansing, MI 48824, USA
[b] Energy and Automotive Research Laboratories (EARL), 1497 Engineering Research Court, Department of Mechanical Engineering, Michigan State University, East Lansing, MI 48824, USA

ARTICLE INFO

Article history:
Received 16 March 2016
Revised 26 August 2016
Accepted 27 August 2016

Keywords:
Diffusion flames
Oscillations
Coflow slot burners
Theoretical analysis
Burke–Schumann model
Infinite-rate chemistry

ABSTRACT

A novel method is presented for solving the forced transient diffusion flame in the exit region of a coflow burner. Streamwise diffusion is eliminated, which produces the Burke–Schumann model. A mathematical transformation renders the transient, forced convection problem equivalent to a steady-state convection problem. The transformation differs from previous approaches because its use does not require a priori restriction to small perturbations. For this reason, flow fluctuations that are large fractions of the initial flow field may be described exactly and features of nonlinear response can be examined without recourse to detailed numerical simulation. The method is applied to study flame evolution and oscillation for two physically separated coflow slot burner flames as they merge.

1. Introduction

In the study of diffusion flames, the Burke–Schumann (B–S) flame model figures prominently as seen in the extensive discussions in [1–3]. The central feature of the B–S model, along with the restriction to infinite-rate chemistry, is the neglect of streamwise diffusion of species, thermal energy and momentum for burner-attached flames. This restriction means that the B–S formulation is a boundary-layer formulation [4]. The neglect of the streamwise component of diffusion renders the problem simpler and easier to solve. This approach has been employed to study many shapes and arrangements of diffusion flames in the science and technology of burner development.

Simplified analytical models provide important physical and mathematical information in the form of quantifiable relationships, which pure numerical models cannot. This is perhaps the principal reason that the studies of Roper [5,6] continue to be referenced in the combustion literature at an unabated rate. In addition, it is the principal reason that numerical simulations of oscillating diffusion flames are discussed and interpreted in terms of simplified theoretical models. The predictions of the former, though limited by their restrictions (e.g., constant properties, infinite-rate chemistry) and simplifications, allow for the interpretation of the solutions of the full equations with variable-properties, multiple-step kinetics, and complex diffusion.

In the past two or three decades, hundreds if not thousands of studies and laboratory trials have been carried out on burner flames.

One important area where diffusion flame oscillations play a role is in the general topic of burner flame attachment. Here, the challenge is to describe the means by which a diffusion flame attaches itself when fuel (or oxidizer) flows through a tube that is surrounded by—or adjacent to—the opposite reactant, namely oxidizer (or fuel). The classical version of this problem [3] describes a jet of fuel ejected into a surrounding, quiescent oxidizer. In this case, the problem may involve turbulence (given a sufficiently large inlet reactant jet Reynolds number) and the associated development of localized shear layers. In order to avoid the fluid mechanical complications caused by vortex trains and coherent structures interlaced with small, intense vortices, researchers have examined jets in which the fuel and surrounding oxidizer have similar velocities. Items of interest are flame heights, combustion rates, flame standoff distances and conditions producing blowoff. Fundamental studies on this topic have been conducted over many years by Chung and co-workers [7,8].

Recent work on oscillating diffusion flames has examined the response of flames to both axial velocity and mixture fraction oscillations [9]. In this work, the mixture fraction equation is solved using perturbation analyses [10] that posit a basic state subjected to flow perturbations. The basic restriction in [9] is to *small* flow perturbations. Thus, the linearized analysis is handicapped because

* Corresponding author.
E-mail addresses: milan@math.msu.edu (M. Miklavčič), wichman@egr.msu.edu (I.S. Wichman).

http://dx.doi.org/10.1016/j.combustflame.2016.08.023
0010-2180/

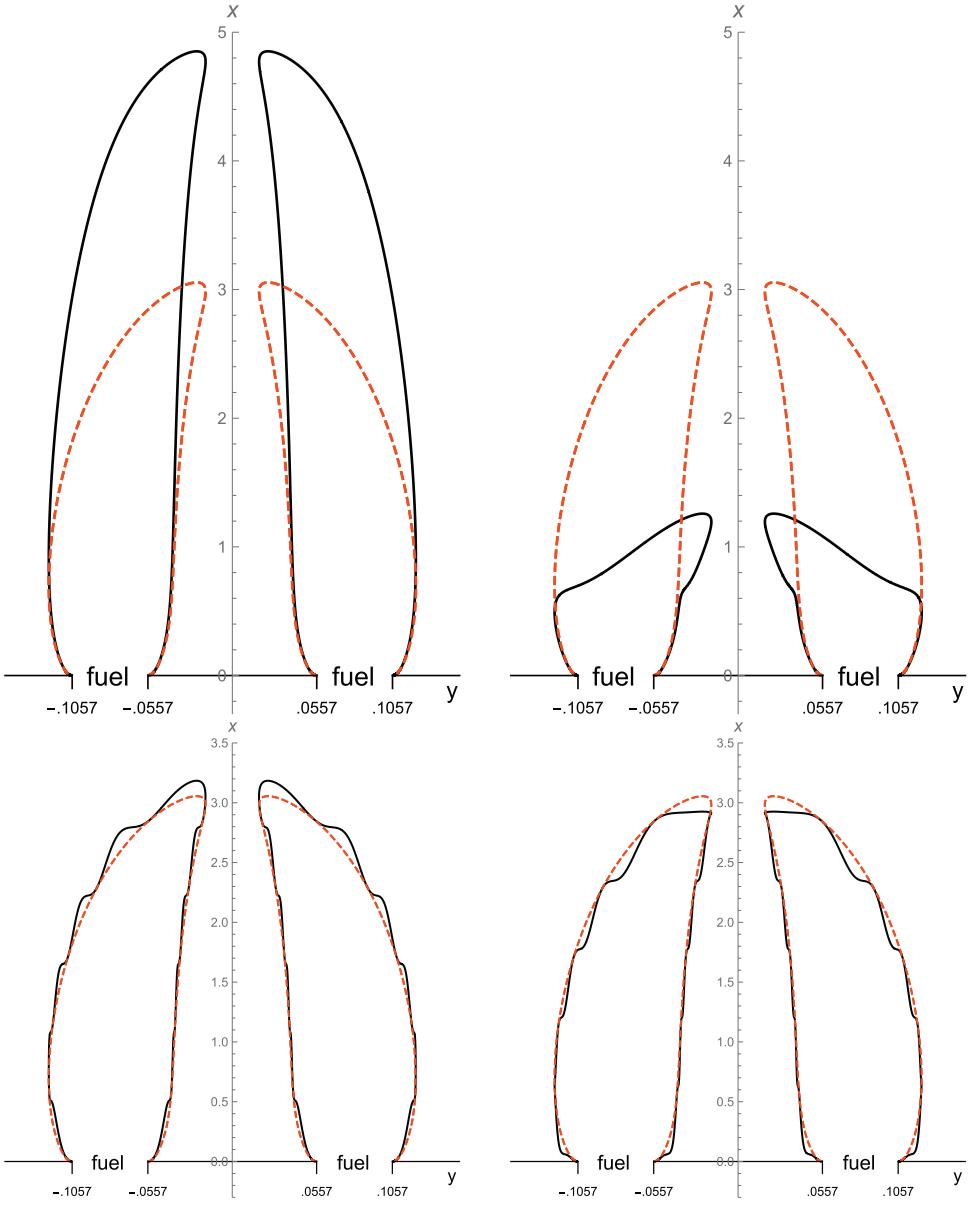

Fig. 1. The burners of width 0.05 are separated by 2 × 0.0557 and the fuel is flowing in x-direction through the fuel slots with the average bulk velocity $u_0 = 100$. The stationary flame corresponding to the average bulk fuel velocity is represented by a dashed line. The bulk fuel velocity is oscillating with amplitude $\varepsilon = 0.9 = 90\%$ of the average velocity u_0 and extrema of the oscillating flame boundaries are represented by solid curves. The circular frequency of oscillations is $\omega = 100$ for the top pair. $\omega = 1100$ for the bottom pair. The diffusion constant is $D = 0.1$. Units and scalings are discussed in Section 4.

the actual process is not linear. As discussed by Takahashi et al. [11], oscillations in the mixture fraction field produce oscillations in the species mixture fractions (oxidizer, fuel) which produces oscillations in the reaction rate (heat release) with resulting oscillations in the temperature field. Oscillation of the temperature field produces larger oscillations in the reaction rate because of its exponential dependence on the temperature. These nonlinear interactions make it impossible for linearized analyses to model processes such as liftoff and blowoff.

2. Problem formulation and transformation

Consider the physical configuration shown in Fig. 1. Here, fuel flows with bulk velocity u toward the positive x-direction through one or more channels that are each adjacent to one or more oxidizer channels. This configuration is called a slot burner, for which experiments have been conducted over many years by many investigators [12,13]. As is explained in detail later in Section 4, this configuration uses a Peclet number of 50, which can be attained in many ways, one of them being a flow velocity of 100 cm/s, a diffusion coefficient of 0.1 cm^2/s and a characteristic length of 0.05 cm. A Peclet number of 50, as will be explained and discussed extensively in Section 4, is entirely in line with previous experiments, hence the values indicated in Fig. 1 are grounded in empirical reality.

Subject to the restriction to equal channel exit velocities, the evolution of the mixture fraction Z for the idealized two-dimensional diffusion flame in the half-space $x \geq 0$ is given by [14,15]

$$\frac{\partial Z}{\partial t} + u\frac{\partial Z}{\partial x} = D\frac{\partial^2 Z}{\partial y^2}. \tag{1}$$

Here, diffusion in the streamwise (x) direction is assumed to be negligible in comparison with streamwise convection term, uZ_x.

This restriction characterizes what is called the unsteady Burke–Schumann flame model [5,14–16].

Consider now the steady case. When $u = u_0 > 0$ is a constant, the burner(s) configuration at $x = 0$ determines the stationary solution Z_0, which satisfies

$$u_0 \frac{\partial Z_0}{\partial x} = D \frac{\partial^2 Z_0}{\partial y^2}. \tag{2}$$

If the solution Z_0 to the steady problem of Eq. (2) is known, then a verification shows that, the solution Z for the corresponding unsteady problem of Eq. (1) is given by

$$Z(x, y, t) = Z_0(u_0(t - S^{-1}(S(t) - x)), y) \qquad \text{for } 0 \le x \le S(t) \tag{3}$$

where the quantity $S(t)$ is defined by

$$S(t) = \int_0^t u(r)\, dr \tag{4}$$

and S^{-1} denotes the inverse of S.

There is only one restriction to this solution. In order for the mathematical relationship in Eq. (3) between Z_0 and Z to exist, the inverse function S^{-1} must exist, i.e., the function $S(t)$ in Eq. (4) must possess the inverse that is required in the solution given by Eq. (3). This requirement demands that the function u in Eq. (4) enable that relationship to be one-to-one. For this to occur it is sufficient that $u = u(t) > 0$, which guarantees the existence of the inverse function. Physically this mathematical constraint means that the fuel is *exiting* the burner and flows downstream.

In [14,15] solutions of Eq. (1) are sought as perturbations of Z_0 when the burner exit velocity u oscillates with small amplitude about a constant value of u_0.

The flame boundary of the infinite-rate chemistry diffusion flame is located at the position where the oxidant and fuel are in the stoichiometric ratio, or in other words, on the contour $Z = Z_{st}$ [5]. Different fuels imply different values of Z_{st}. In our computations we use $Z_{st} = 0.3$, as in [14]. We let $y = \xi(x, t)$ be a local representation of the flame boundary, where let $y = \xi_0(x)$ is the local representation of the stationary flame boundary. Hence, the flame location is given by the relationship

$$Z_{st} = Z(x, \xi(x, t), t) = Z_0(\eta, \xi_0(\eta)).$$

For a point (x, y) on the boundary of the flame at time t, the flame position relationship requires that $Z(x, y, t) = Z_{st}$ and if we define the modified spatial variable

$$\eta = u_0(t - S^{-1}(S(t) - x)), \tag{5}$$

we see that Eq. (3) implies that $Z_0(\eta, y) = Z_{st}$. Hence, (η, y) is also on the boundary of the stationary flame. From the definitions of ξ_0, ξ we have that $y = \xi_0(\eta) = \xi(x, t)$ and therefore the transient flame boundary is related to the stationary flame boundary as follows:

$$\xi(x, t) = \xi_0(\, u_0(t - S^{-1}(S(t) - x))). \tag{6}$$

Conversely, for any boundary point of a stationary flame $(\eta, \xi_0(\eta))$ we can solve Eq. (5) for x giving

$$x = S(t) - S(t - \eta/u_0) = \int_0^{\eta/u_0} u(t - r)\, dr, \quad y = \xi_0(\eta) \tag{7}$$

which equations satisfy $Z(x, y, t) = Z_0(\eta, y) = Z_{st}$. Hence the point (x, y) is indeed on the temporal flame boundary at time t.

For diffusion flames, the reactant consumption rate is proportional to the flame area which, for the slot burner configuration, is instantaneously proportional to the length of the arc defined by $Z(x, y, t) = Z_{st}$. For each branch the length of the curve is given by

$$\int \sqrt{1 + \left(\frac{\partial \xi}{\partial x}\right)^2}\, dx = \int \sqrt{\left(\frac{\partial x}{\partial \eta}\right)^2 + \left(\frac{d\xi_0}{d\eta}\right)^2}\, d\eta \tag{8}$$

which simplifies to

$$\int \sqrt{\left(\frac{u(t - \eta/u_0)}{u_0}\right)^2 + \left(\xi_0'(\eta)\right)^2}\, d\eta. \tag{9}$$

after using Eq. (7). The evaluation of this integral provides the flame surface area.

Finally, when u has period T and average value u_0, Eq. (7) implies that the flame boundary oscillates in the x-direction around the locus η, also with period T. Moreover, $Z(x, y, t + T) = Z(x, y, t)$.

3. Special case: sinusoidally oscillating flow field

In several studies [14,15] it is assumed that the bulk flow field oscillates as

$$u = u_0 + \varepsilon u_0 \cos \omega t. \tag{10}$$

Hence, we have $S(t) = u_0 t + (\varepsilon u_0 \sin \omega t)/\omega$ and Eq. (7) implies that the flame boundary point at $y = \xi_0(\eta)$ oscillates in the x-direction around the steady value η according to the transformed relationship

$$x = \eta + \frac{\varepsilon u_0}{\omega}\left(\sin \omega t - \sin \omega\left(t - \frac{\eta}{u_0}\right)\right) \tag{11}$$

$$= \eta + \varepsilon \eta \frac{\sin \delta}{\delta} \cos(\omega t - \delta), \quad \text{where } \delta = \frac{\omega \eta}{2u_0}. \tag{12}$$

Note that the flame does not oscillate when $\delta = k\pi$, which defines nodal planes $\eta = k u_0 2\pi/\omega$ for $k = 1, 2, \ldots$ Here we only need to satisfy the constraint $|\varepsilon| < 1$ (which guarantees that the bulk velocity of the coflowing stream is always *downstream*) to ensure that Z given by Eq. (3) is well defined.

In previous studies [14,15] it is assumed that $|\varepsilon|$ is much smaller than unity. Then, linearizations of Z and ξ with respect to ε are found for a particular burner configuration and the corresponding Z_0.

These linearized solutions can be obtained as follows for the present nonlinear formulation very simply for arbitrary steady state solutions Z_0. First note that

$$S^{-1}(r) = \frac{r}{u_0} - \frac{\varepsilon}{\omega} \sin \frac{\omega r}{u_0} + O(\varepsilon^2). \tag{13}$$

Hence we obtain

$$u_0(t - S^{-1}(S(t) - x)) = x - \frac{\varepsilon u_0}{\omega}\left(\sin \omega t - \sin \omega\left(t - \frac{x}{u_0}\right)\right) + O(\varepsilon^2). \tag{14}$$

Eqs. (3) and (14) imply the linearization

$$Z(x, y, t) = Z_0(x, y) - \frac{\varepsilon u_0}{\omega}\left(\sin \omega t - \sin \omega\left(t - \frac{x}{u_0}\right)\right)\frac{\partial Z_0}{\partial x}(x, y) + O(\varepsilon^2), \tag{15}$$

which agrees with Eq. (14) of [14]. Eqs. (6) and (14) also imply the linearization

$$\xi(x, t) = \xi_0(x) - \frac{\varepsilon u_0}{\omega}\left(\sin \omega t - \sin \omega\left(t - \frac{x}{u_0}\right)\right)\xi_0'(x) + O(\varepsilon^2), \tag{16}$$

which corresponds to Eq. (20) in [14], which is considered to be a key contribution of [14]. Eq. (15) provides a good approximation for Z when $|\varepsilon| \ll 1$. Eq. (3), however, is an *exact* solution of Eqs. (1) and (10).

Numerically, the computation of S^{-1} in the exact solution can be made nearly as efficient as the computation of S when using Eq. (10). Likewise, Eq. (16) also provides a good approximation for

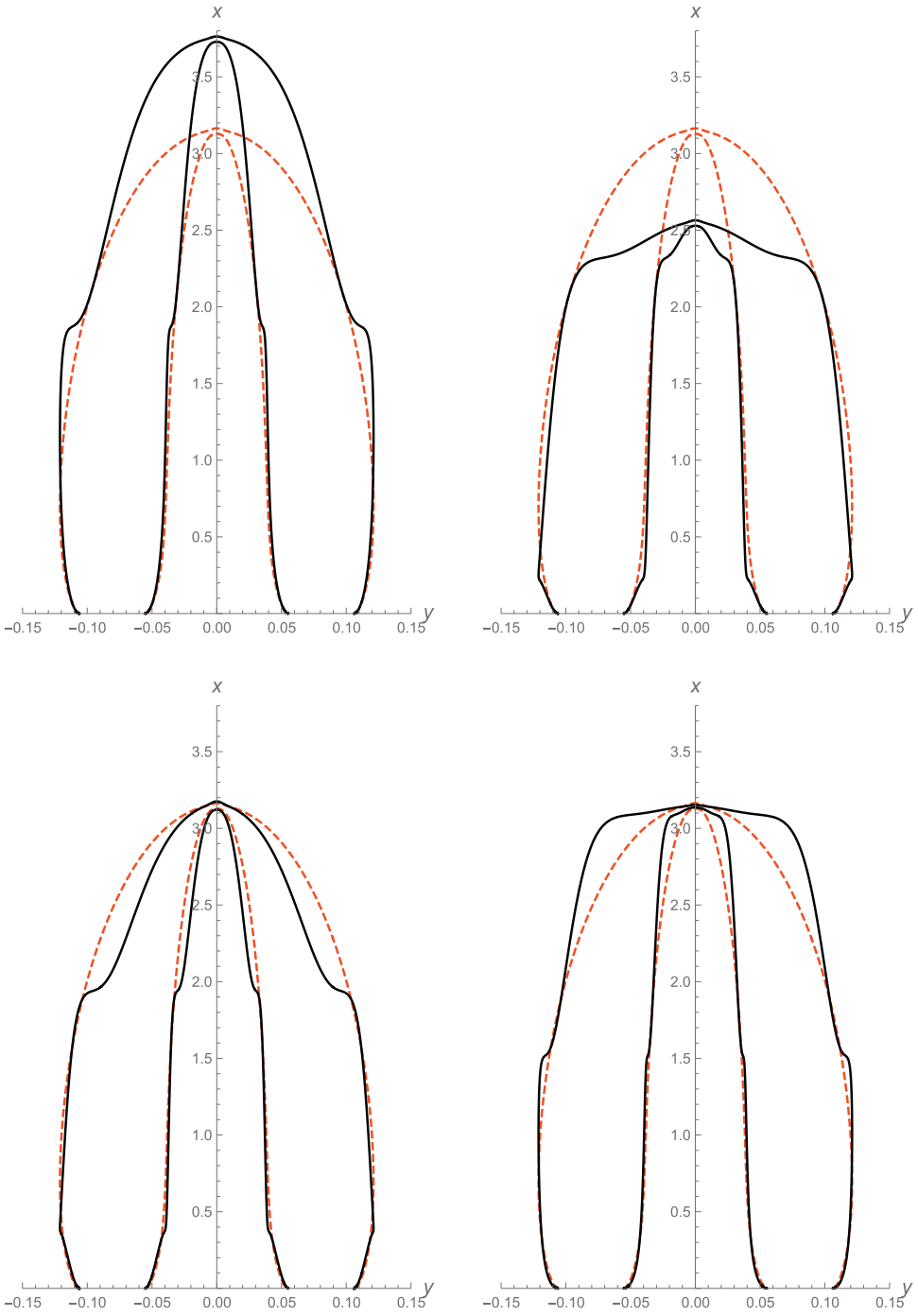

Fig. 2. The burners of width 0.05 are separated by 2 × 0.055665, $u_0 = 100$, $\varepsilon = 0.9$, $D = 0.1$. $\omega = 300$ for the top pair. $\omega = 400$ for the bottom pair.

the transient behavior of the flame boundary when $|\varepsilon| \ll 1$. However, our Eqs. (6) and (11) describe the flame boundary exactly.

When the bulk velocity u is given by Eq. (10) the dynamic reaction zone of Eq. (9) is proportional to the sum of the following integrals:

$$\int \sqrt{\left(1 + \varepsilon \cos\omega\left(t - \frac{\eta}{u_0}\right)\right)^2 + \left(\xi_0'(\eta)\right)^2}\, d\eta \tag{17}$$

evaluated over all the branches of the stationary flame boundary.

4. Merger of two coflow slot flames

The problem of merging diffusion flames, which has been studied experimentally [17–19], gives us an opportunity to easily study large flame oscillations with the tools developed in the preceding sections.

Consider a burner with one slot delivering fuel between locations L_1 and L_2 along the y-axis (see Fig. 1) and another slot between the locations $-L_2$ and $-L_1$. As in [14,15], we assume periodicity in the y-direction, with period $2L$. Since $Z_0(0, y) = 1$ at the exit plane for coordinate y in the two slots delivering fuel and $Z_0(0, y) = 0$ at the exit plane for all other values of coordinate y, the stationary solution of Eq. (2) corresponding to this burner

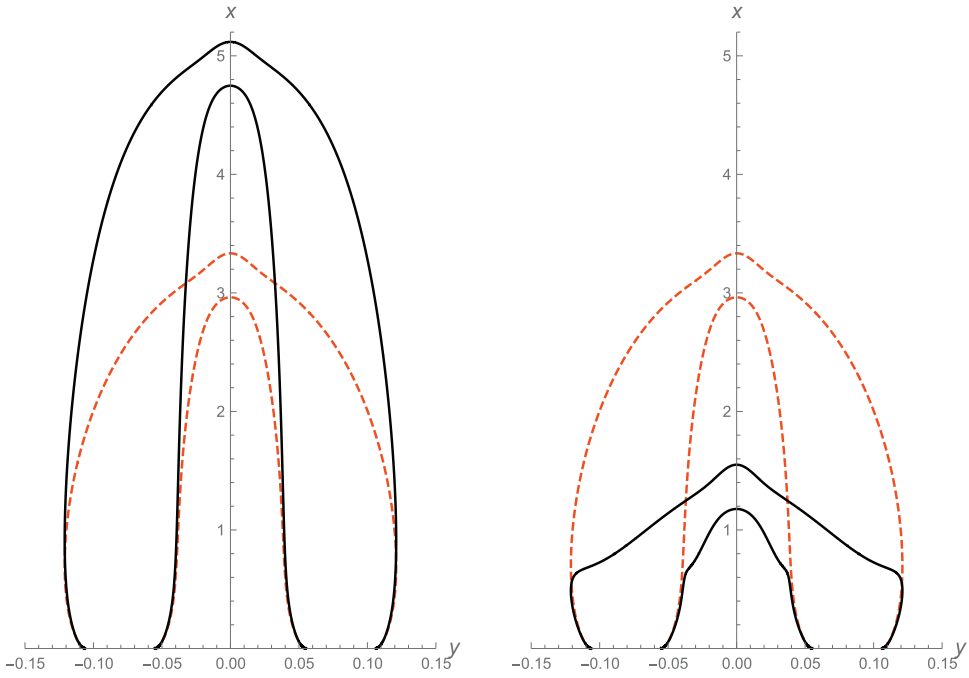

Fig. 3. The burners of width 0.05 are separated by 2 × 0.0556, $u_0 = 100$, $D = 0.1$, $\omega = 100$, $\varepsilon = 0.9$. Flame contours at the times when their lengths are maximal (19.75) and minimal (5.48).

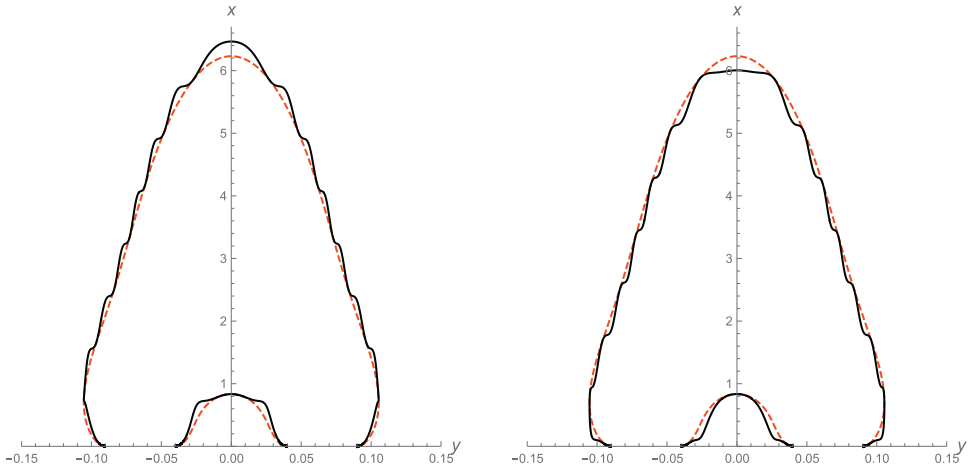

Fig. 4. The burners of width 0.05 are separated by 2 × 0.04, $u_0 = 100$, $D = 0.1$, $\varepsilon = 0.9$, $\omega = 750$.

configuration is equal to

$$Z_0(x,y) = \frac{L_2 - L_1}{L} + \sum_{n=1}^{\infty} \frac{2}{n\pi}\left(\sin\frac{n\pi L_2}{L} - \sin\frac{n\pi L_1}{L}\right) \times e^{-\frac{(n\pi)^2 D}{L^2 u_0}x} \cos\frac{n\pi y}{L}. \tag{18}$$

Note that if $L_1 = 0$ then we have just one burner and Eq. (18) gives in this case the same Z_0 as is used in [1,14]. In order to avoid interference with other burners in the periodic structure, we choose L_2 and L_1 to be small compared to L. If we would choose just two burners, with no periodicity, then the corresponding solution of Eq. (2) would be given by

$$2Z_0(x,y) = \operatorname{erf}\frac{L_2 - y}{\sqrt{4xD/u_0}} + \operatorname{erf}\frac{y - L_1}{\sqrt{4xD/u_0}} + \operatorname{erf}\frac{y + L_2}{\sqrt{4xD/u_0}} - \operatorname{erf}\frac{L_1 + y}{\sqrt{4xD/u_0}}. \tag{19}$$

where

$$\operatorname{erf} y = \frac{2}{\sqrt{\pi}}\int_0^y e^{-r^2}\,dr.$$

For the range of parameters used, the flame contours $Z_0 = Z_{st} = 0.3$ given by Eq. (19) are, for all practical purposes, the same as those given by Eq. (18).

We consider now the scaling of the burner widths, the flow speed and the physical coefficients. The Peclet number, which is the dimensionless ratio of convection to mass diffusion, is taken to be an order of magnitude larger than unity without becoming large enough to produce turbulence. We take $Pe = u_0(L_2 - L_1)/D = 50$ (in the range of experimental studies [20]). This is achieved by several means as will now be described:

(1) In order to obtain $Pe = 50$ we choose a velocity of $u_0 = 100$, a characteristic length of $L = 0.05$ and a diffusion coefficient $D = 0.1$. This can be achieved either by adjusting the scale of the physical variables, as was discussed in the caption to Fig. 1, or by noticing that these values are nearly those used in experiments,

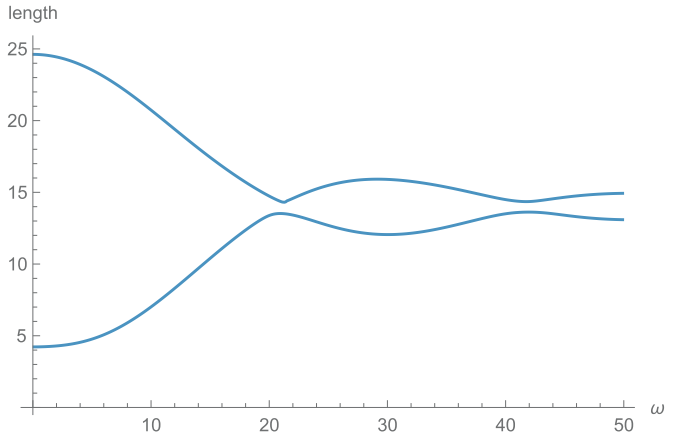

Fig. 5. Maximum and minimum lengths of the boundary of the flame at $\varepsilon = 0.9$. The burners of width 0.5 are separated by 2×0.556, $u_0 = 10$, $D = 1$. When $\omega = 10$ the maximum length is 20.73, the minimum length is 7.01 and the flames look just like those on Fig. 3 but with y axis values 10 times larger.

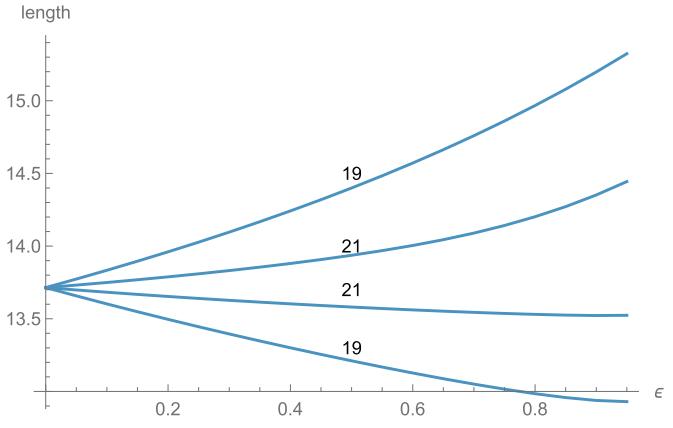

Fig. 6. Maximum and minimum lengths of the boundary of the flame at $\omega = 19$ and $\omega = 21$. The burners of width 0.5 are separated by 2×0.556, $u_0 = 10$, $D = 1$. At $\varepsilon = 0$ the length is 13.71.

$u_0 = 100$ cm/s, $L = 0.05$ cm, $D = 0.1\,\text{cm}^2/\text{s}$. Either way, the value $Pe = 50$ is attained. Note in this particular case that the characteristic length is very small and therefore as mentioned the flames are long but separated.

(2) Here the goal is to produce flames that are not as narrow. Hence the length scale is expanded and the velocity is reduced. Choose the length scale so that $L = 0.5$ (say, 0.5 cm) and then choose $u_0 = 10$ (say, 10 cm/s) and $D = 1$ (say $1\,\text{cm}^2/\text{s}$). This gives the smaller value $Pe = 5$ which produces slower and wider flames.

(3) In terms of standard physical variables, if the inflowing gases have properties similar to air, then at standard temperature and pressure we have $D = 0.2\,\text{cm}^2/\text{s}$. For a burner having characteristic width 0.5 cm an exit velocity of 20 cm/s gives $Pe = 50$. Shrinking the length scale by a factor of five while increasing the flow velocity by the same factor preserves the Peclet number and essentially yields case (1) above.

We use u as given by Eq. (10) with $\varepsilon = 0.9$ in all of our calculations. Therefore linearizations [9,14] are not applicable. The Strouhal number, which is the dimensionless ratio of the characteristic flow time to the oscillation time based on the width of the burner slot, is defined as $St_w = \omega(L_2 - L_1)/(2\pi u_0)$ and ranges between .01 and 1 in our computations.

We have performed direct computations of flame contours at different times using Eq. (3). However, to resolve the details near the merger point, as on Fig. 2, these computations can be very time consuming and perhaps even not doable without our transformation Eq. (3). A much more efficient way to compute accurate dynamic flame contours $Z(x, y, t) = Z_{st}$ is to first compute contours of the stationary flame accurately, then to extract coordinate pairs $(\eta, \xi_0(\eta))$ that determine the boundary of the stationary flame and

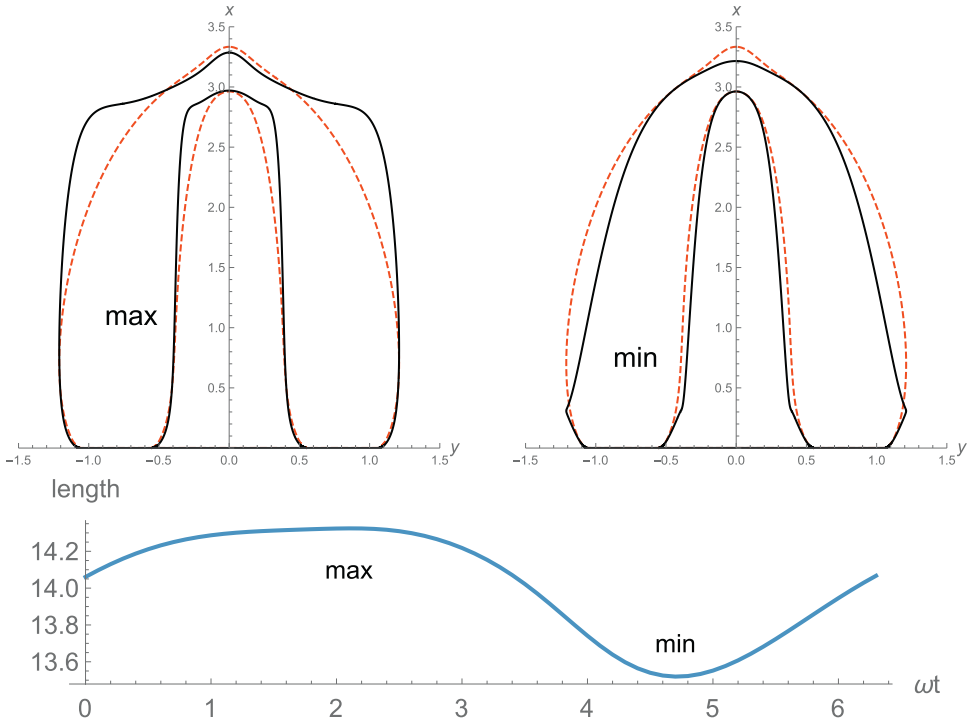

Fig. 7. Variation of the length of the boundary of the flame with time when $\omega = 21.1$. The burners of width 0.5 are separated by 2×0.556, $u_0 = 10$, $D = 1$.

finally use Eq. (11) (for the bulk sinusoidally oscillating flow field case) to obtain the dynamic flame contours.

Figure 1 shows the two burners separated by 2×0.0557. The flames are separate but tip toward, or "attract", each other. The tipping is especially pronounced at lower frequencies as shown by the upper pair of flames at two different times. This observation may suggest the following question. Is it possible that at a certain separation distance the flames are joined for one part of the cycle and separated for the other part? This certainly seems plausible based on observations of real chaotic flames, however it is not possible in our ideally controlled set up because of the following. Whenever a stationary flame is joined its boundary oscillates according to Eq. (12) – it cannot break. In Fig. 1 the distance between the flames does not change with time.

To see what happens when the burners are brought together just enough for the flames to join, consider Fig. 2. The flames are joined when $L_1 \leq 0.055665$ and they are separate when $L_1 \geq 0.055666$. At the tip of the stationary flame $\eta = 3.1$, hence $\omega\eta/u_0 \approx 4\pi$ when $\omega = 400$, and hence the tip of the flame is approximately on the second nodal plane and therefore it barely oscillates. This is illustrated by the bottom pair of flame contours computed at two different times. When $\omega = 300$, then $\omega\eta/u_0 \approx 3\pi$ and the tip of the flame oscillates between the first and the second nodal planes as illustrated by the top pair at two different times. The same pattern is repeated for larger ω but the amplitude of oscillations decreases with ω. This is demonstrated by the bottom pair at $\omega = 1100$ in Fig. 1.

Figure 3 shows the two burners separated by 2×0.0556. The flames are joined at this separation distance. If the burners are moved even closer together, like on Fig. 4 where they are separated by 2×0.04, the flame shapes very much resemble those in [9]. Note also, that the flame height increases as the burners get closer which of course agrees with experiments [17,18]. For single long slot burners the flame height is proportional to the square of the slot size [5], hence, the height of the flame when the two burners are joined is four times as large as when they are far apart.

This preceding range of parameters creates thin, high flames, hence the reaction zone, which is proportional to the length of the boundary of the flame, is nearly proportional to the flame height for the above cases.

In order to illustrate features of flame length variation more clearly, we consider a rescaled version of the problem in which $Pe = 5$, $u_0 = 10$, $L_2 - L_1 = 0.5$, $D = 1$ and the burners are 2×0.556 apart. This creates flames just like those on Fig. 3 but with y-axis values larger by factor of ten at frequencies that are ten times smaller. The length of the flame boundary, which is proportional to the reactant consumption rate, oscillates about the length of the stationary flame (13.71); see Fig. 7. We calculated the maximum and the minimum lengths of the flame boundary for a range of values of ω and ε. Results appear in Figs. 5 and 6. As ω increases the difference between the maximum and minimum value of the length decreases till $\omega_1 = 21.1$ at which point the difference is 0.81. See Fig. 7 and note the asymmetry between time spent near the maximum length and time spent near the minimum length at this frequency. This asymmetry is a nonlinear effect. Figure 5 looks approximately how one would expect based on Eq. (12). The second minimum occurs at $\omega_2 = 41.8$ which is roughly, but not exactly, equal to $2\omega_1$. Figure 6 also suggests that nonlinear effects are more significant at the minima.

5. Summary and conclusions

A mathematical transformation of the steady or basic state solution of the coflow burner flame model (Section 2) permits a careful, exact analysis of the problem both numerically (computation) and conceptually (interpretation and evaluation of the results). Two examples were considered, the sinusoidally oscillating flame examined by previous investigators Section 3) and the oscillating merged flames of Section 4 [21]. In both cases, a linearized limit is obtained but, unlike previous analyses, the *nonlinear response* can also be analyzed. As shown in Section 4, the nonlinear response displays features that cannot be captured by the linear analysis such as asymmetries in the fluctuation process. This may have practical implications when the full forcing and response spectra need to be analyzed.

References

[1] S.P. Burke, T.E.W. Schumann, Diffusion flames, Ind. Eng. Chem. 29 (1928) 998–1004.
[2] F.A. Williams, Combustion theory, Benjamin-Cummings, Menlo Park, 1985.
[3] C.K. Law, Combustion physics, Cambridge University Press, NY, 2006.
[4] H. Schlichting, K. Gersten, Boundary layer theory, 8th ed., Springer Press, 2000.
[5] F.G. Roper, The prediction of laminar jet diffusion flame sizes: Part I. Theoretical model, Combust. Flame 29 (1977) 219–226.
[6] F.G. Roper, The prediction of laminar jet diffusion flame sizes: Part II. Experimental verification, Combust. Flame 29 (1977) 227–234.
[7] S.H. Chung, B.J. Lee, On the characteristics of laminar lifted flames in a nonpremixed jet, Combust. Flame 86 (1991) 62.
[8] J. Lee, S.H. Won, S.H. Jin, S.H. Chung, Lifted flames in laminar jets of propane in coflow air, Combust. Flame 135 (2003) 449–462.
[9] K. Preetham, H. Thumuluru, T.L. Santosh, Linear response of laminar premixed flames to flow oscillations: unsteady stretch effects, J. Propuls. Power 26 (2010) 524–532.
[10] T. Lieuwen, Unsteady combustor physics, Cambridge University Press, NY, 2012.
[11] F. Takahashi, G.T. Linteris, V.R. Katta, Vortex-coupled oscillations of edge diffusion flames in coflowing air with dilution, Proc. Combust. Inst. 31 (2007) 1575–1582.
[12] A.G. Gaydon, H.G. Wolfhard, Flames: their structure, radiation and temperature, 4th ed., Chapman and Hall, London, 1979.
[13] R. Azzoni, S. Ratt, S.K. Aggrawal, I.K. Puri, The structure of triple flames stabilized on a slot burner, Combust. Flame 119 (1999) 23–40.
[14] N. Magina, D. Shin, V. Acharya, T. Lieuwen, Response of non-premixed flames to bulk flow perturbations, Proc. Combust. Inst. 34 (2013) 963–971.
[15] M. Tyagi, N. Jamadar, S.R. Chakravarthy, Oscillatory response of an idealized two-dimensional diffusion flame: analytical and numerical study, Combust. Flame 149 (2007) 271–285.
[16] S.S. Krishnan, J.M. Abshire, P.B. Sunderland, Z.G. Yuan, J.P. Gore, Analytical predictions of shapes of laminar diffusion flames in microgravity and earth gravity, Combust. Theory Model. 12 (2008) 605–620.
[17] O. Sugawa, Y. Oka, Experimental study on flame merging behavior from 2 by 3 configuration model fire sources, Fire Saf. Sci. 7 (2003) 891–902.
[18] S. Schälike, K.B. Mishra, K.-D. Wehrstedt, A. Schönbucher, Limiting distances for flame merging of multiple n-heptane and di-tert-butyl peroxide pool fires, Chem. Eng. Trans. 32 (2013) 121–126.
[19] H.F. Yang, C.M. Hsu, R.F. Huang, Flame behavior of bifurcated jets in a V-shaped bluff-body burner, J. Mar. Sci. Technol. 22 (2014) 606–611.
[20] C. Miesse, R.I. Maisel, M. Short, M.A. Shannon, Diffusion flame instabilities in a 0.75 mm nono-premixed microburner, Proc. Combust. Inst. 30 (2005) 2499–2507.
[21] F.G. Roper, Laminar diffusion flame sizes for interacting burners, Combust. Flame 34 (1979) 19–27.